Frequency and intensity of palaeofloods at the interface of Atlantic and Mediterranean climate domains

B. Wilhelm, H. Vogel, C. Crouzet, David Etienne, F. S. Anselmetti

Clim. Past, 12, 299–316, 2016
www.clim-past.net/12/299/2016/
doi:10.5194/cp-12-299-2016

Climate of the Past
Open Access
EGU

Frequency and intensity of palaeofloods at the interface of Atlantic and Mediterranean climate domains

B. Wilhelm[1,2], **H. Vogel**[2], **C. Crouzet**[3,4], **D. Etienne**[5], **and F. S. Anselmetti**[2]

[1]Université Grenoble Alpes, LTHE, 38000 Grenoble, France
[2]Institute of Geological Sciences and Oeschger Centre for Climate Change Research, Univ. of Bern, 3012 Bern, Switzerland
[3]Université Savoie Mont Blanc, ISTerre, 73376 Le Bourget-du-Lac, France
[4]CNRS, ISTerre, 73376 Le Bourget-du-Lac, France
[5]UMR INRA 42 CARRTEL, Université Savoie Mont Blanc, 73376 Le Bourget-du-Lac, France

Correspondence to: B. Wilhelm (bruno.wilhelm@ujf-grenoble.fr)

Received: 22 September 2015 – Published in Clim. Past Discuss.: 23 October 2015
Revised: 3 February 2016 – Accepted: 4 February 2016 – Published: 17 February 2016

Abstract. The long-term response of the flood activity to both Atlantic and Mediterranean climatic influences was explored by studying a lake sequence (Lake Foréant) of the Western European Alps. High-resolution sedimentological and geochemical analysis revealed 171 event layers, 168 of which result from past flood events over the last millennium. The layer thickness was used as a proxy of intensity of past floods. Because the Foréant palaeoflood record is in agreement with the documented variability of historical floods resulting from local and mesoscale, summer-to-autumn convective events, it is assumed to highlight changes in flood frequency and intensity related to such events typical of both Atlantic (local events) and Mediterranean (mesoscale events) climatic influences. Comparing the Foréant record with other Atlantic-influenced and Mediterranean-influenced regional flood records highlights a common feature in all flood patterns that is a higher flood frequency during the cold period of the Little Ice Age (LIA, AD 1300–1900). In contrast, high-intensity flood events are apparent during both the cold LIA and the warm Medieval Climate Anomaly (MCA, AD 950–1250). However, there is a tendency towards higher frequencies of high-intensity flood events during the warm MCA. The MCA extremes could mean that under the global warming scenario, we might see an increase in intensity (not in frequency). However, the flood frequency and intensity in the course of the 20th century warming trend did not change significantly. Uncertainties in future evolution of flood intensity lie in the interpretation of the lack of 20th century extremes (transition or stable?) and the different climate forcing factors between the two periods (greenhouse gases vs. solar and/or volcanic eruptions).

1 Introduction

Heavy rainfall events trigger mountain-river floods, one of the most significant natural hazards, causing widespread loss of life, damage to infrastructure and economic deprivation (e.g. Kundzewicz et al., 2014). This is especially the case for the Alpine area in Europe, where tourism and recent demographic development with an increasing population raise the vulnerability of infrastructure to natural hazards (e.g. Beniston and Stephenson, 2004). Moreover, the current global warming is expected to lead to an intensification of the hydrological cycle and a modification of flood hazard (IPCC et al., 2013). Hence, a robust assessment of the future evolution of the flood hazard over the Alps becomes a crucial issue.

A main limitation for robust flood-hazard projections is the scarce knowledge on the underlying natural climate dynamics that lead to these extreme events (IPCC, 2013). Indeed, the stochastic nature and the rare occurrence of extreme events make the identification of trends based on instrumental data alone difficult (e.g. Lionello et al., 2012). One way of overcoming this issue is to extend flood series beyond observational data and compare these data sets with independent climatic and environmental forcing. In this purpose, many types of sedimentary archives have been studied (e.g. Lutterbacher et al., 2012 and references therein). Among them lake

sediments are being increasingly studied because they allow to reconstruct flood records long enough to identify the natural variability at different timescales (e.g. Noren et al., 2002; Oslegger et al., 2009; Wilhelm et al., 2012a; Czymzik et al., 2013; Glur et al., 2013; Corella et al., 2014).

In the western Alps, many lake-sediment sequences have been studied to better assess the response of the flood activity to climate variability. These studies revealed higher flood frequency of mountain streams in many regions during multicentennial cold phases such as the Little Ice Age (Giguet-Covex et al., 2012; Wilhelm et al., 2012a, 2013; Glur et al., 2013; Wirth et al., 2013b; Amann et al., 2015). However, regarding flood intensity and/or magnitude, opposite patterns appear with the occurrence of the most extreme events during warmer periods in the north (Giguet-Covex et al., 2012; Wilhelm et al., 2012b, 2013), while they occurred during colder periods in the south (Wilhelm et al., 2012a, 2015). These north-south opposite flood patterns were explained by flood-triggering meteorological processes specific to distinct climatic influences: Atlantic in the north versus Mediterranean in the south. In the north-western part of the Alps, floods at high altitude are mainly triggered by local convective events (i.e. thunderstorms) and seem to mainly depend on the temperature that would strengthen vertical processes (e.g. Wilhelm et al., 2012b, 2013). In contrast, floods in the south are mostly triggered by mesoscale events and may strongly depend on pathways and intensity of storm-tracks (e.g. Trigo and Davis, 2000; Boroneant et al., 2006; Boudevillain et al., 2009). By analogy with these results over past warm periods, the mountain-flood hazard might be expected to increase in the north-western Alps, mainly because of an enhanced flood magnitude associated to stronger convective processes. Hence, better assessing the spatial extent of the Atlantic-influenced flood pattern at high-altitude appears a crucial issue to appropriately establish hazard mitigation plans and prevent high socio-economic damages.

In this context, the present study was designed to reconstruct the flood pattern at an intermediate situation between the north-western and south-western Alps, i.e. at the climate boundary between Atlantic and Mediterranean influences. This is undertaken by reconstructing a millennium-long flood chronicle from the sediment sequence of the high-altitude Lake Foréant located in the Queyras Massif (France).

2 Regional setting

2.1 Hydro-climatic setting and historical flood record

The Queyras massif is located in between the northern and southern French Alps where the climate is influenced by the Atlantic Ocean and the Mediterranean Sea (Fig. 1). As a result, the Queyras mountain range corresponds to a transition zone of Alpine precipitation patterns in the meteorological reanalyses (Durant et al., 2009; Plaut et al., 2009) and in the simulations (Frei et al., 2006; Rajczak et al., 2013). In the Queyras, heavy precipitation events are related to either local convective phenomena (i.e. summer thunderstorms) or mesoscale convective systems. The mesoscale systems called "Lombarde-Type" or "East Return" events occur mainly from late spring to autumn and result from Mediterranean humid air masses flowing northward into the Po Plain and then westward to the Queyras Massif (e.g. Gottardi et al., 2010; Parajka et al., 2010). The humid air masses are then vigorously uplifted with the steep topography of the Queyras massif, causing an abrupt cooling of the air masses and intense precipitations. Such mesoscale precipitation events, typical of the Mediterranean climate (e.g. Buzzi and Foschini, 2000; Lionello et al., 2012), affect extensive areas and may lead to catastrophic floods at a regional scale as shown in June 1957 or October 2000 over the Queyras massif (Arnaud-Fassetta and Fort, 2004). Other numerous past flood events were documented from studies of local historical records. These data have been compiled in a database managed by the ONF-RTM (http://rtm-onf.ifn.fr/). They show that the village of Ristolas (located 8 km downstream from Lake Foréant, Fig. 1c) has been affected at least 34 times over the last 250 years by floods of the Guil River and its five main tributaries (see Supplement).

2.2 Lake Foréant and its tributaries

Lake Foréant (2620 m a.s.l., 44°42′20″ N, 6°59′00″ E) is located in a cirque of 3 km^2 in the upper part of the Queyras Massif, adjacent to the Italian border (Fig. 1). It is located approximately 60 km north from Lake Allos and 100 km south-west from Lake Blanc, whose hydro-climatic settings are characterized by the south-western and north-western flood pattern, respectively (Wilhelm et al., 2012a, b; Fig. 1b). The catchment rises up to 3210 m. a.s.l. and is made up of three lithologies from the Queyras schistes-lustrés nappe (e.g. Schwartz et al., 2009); (i) marble in the eastern part, (ii) calc-schist in the western part and (iii) a narrow band of arkose in between (Fig. 1d). The main stream of the catchment, the Torrent de Bouchouse, drains mainly the central band of arkose. Before entering the lake, this stream has built an alluvial plain (Fig. 1e). This suggests that the Bouchouse stream is a major source of sediment entering the lake. In addition, two minor and non-permanent streams drain the western part of the catchment. In contrast, they enter the lake through only small deltas compared to the Bouchouse inflow area, suggesting limited detrital inputs. There is no evidence that the catchment was glaciated in the past, i.e. no moraine or other glacial deposits occur. Thereby, detrital inputs only result from the erosion and transport of these lithologies. Detrital inputs from these streams are limited to summer and autumn because the catchment is covered by snow and the lake is frozen from mid-November to the beginning of June. The Bouchouse stream flows downstream into the Guil River and reaches approximately 8 km further the village of Ristolas (Fig. 1c).

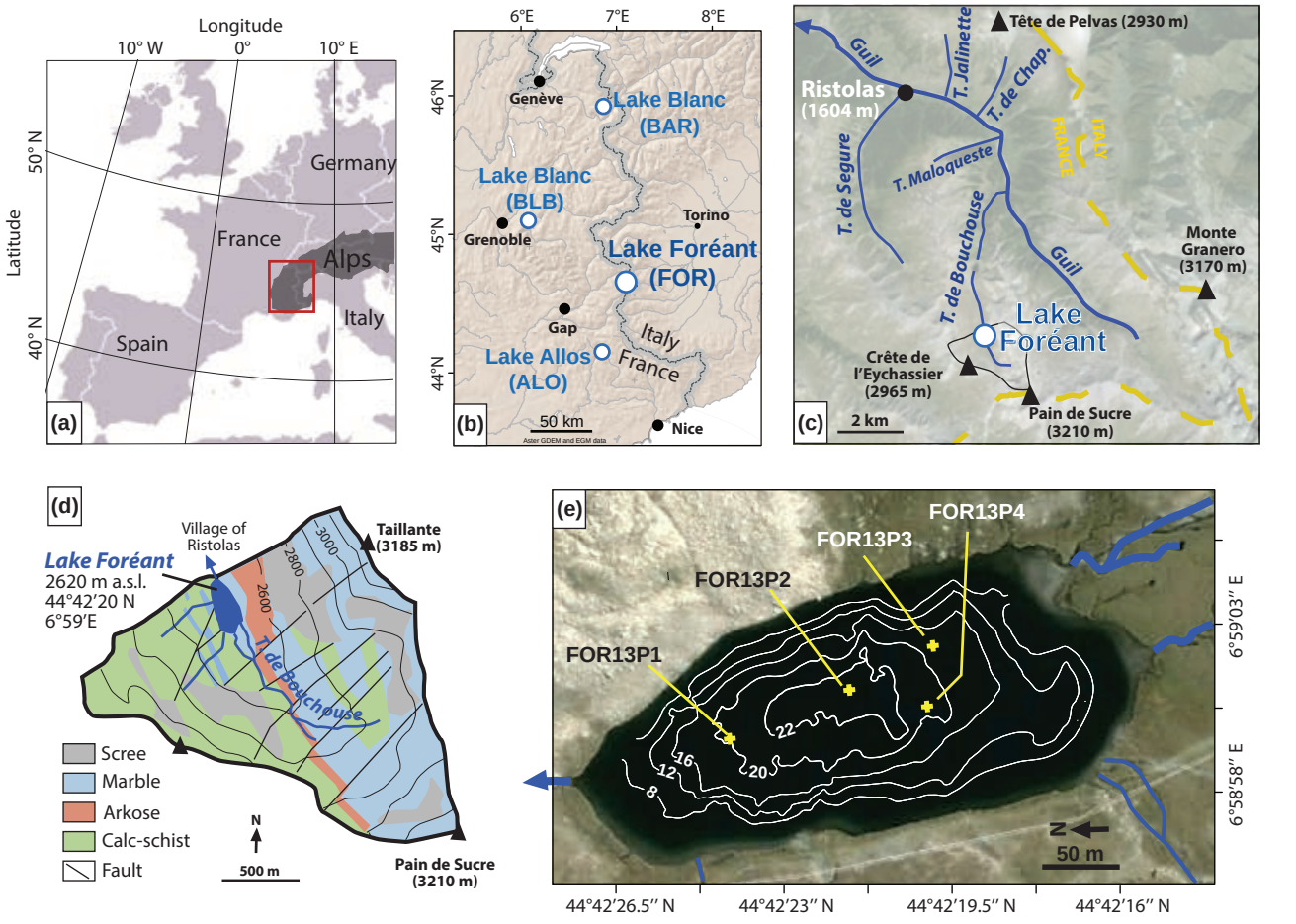

Figure 1. **(a)** Location of Lake Foréant in the western Alps, **(b)** compared to the locations of the previously studied Lake Blanc (BLB, Wilhelm et al., 2012b; BAR, Wilhelm et al., 2013) and Lake Allos (ALO, Wilhelm et al., 2012a). **(c)** Location of the Foréant catchment area in the hydrological network flowing to the village of Ristolas. **(d)** Geological and geomorphological characteristics of the Foréant catchment area. **(e)** Bathymetric map of Lake Foréant and coring sites.

3 Method

3.1 Lake coring

In summer 2013, a bathymetric survey was carried out on Lake Foréant and revealed a well-developed flat basin in the centre of the lake with a maximum water depth of 23.5 m (Fig. 1e). An UWITEC gravity corer was used to retrieve four cores along a north-south transect in the axis of the two main inlets of the Bouchouse stream. Cores FOR13P3 and FOR13P4 correspond to the proximal locations of the two different branches of the Bouchouse stream and aim at investigating their respective sediment inputs during floods. Cores FOR13P2 and FOR13P1 correspond to the depocenter and to the most distal position, i.e. the opposite slope to the Bouchouse inflows, respectively.

3.2 Core description and logging

Cores were split lengthwise and the visual macroscopic features of each core were examined to identify the different sedimentary lithofacies. The stratigraphic correlation between the cores was then carried out based on these defined lithofacies. The stratigraphic correlation allows identifying the depositional pattern of the event layers within the lake basin. Depositional patterns of event layers may help to decipher their trigger, i.e. mass-movements vs. flood events (e.g. Sturm and Matter, 1978; Wilhelm et al., 2012b; Van Daele et al., 2015).

High-resolution colour line scans and gamma-ray attenuation bulk density measurements were carried out on a GeotekTM multisensor core-logger (Institute of Geological Sciences, University of Bern). Bulk density was used as a proxy of event layers, e.g. flood layers, characterized by higher density due to the high amount of detrital material

(e.g. Støren et al., 2010; Gilli et al., 2012; Wilhelm et al., 2012b).

Geochemical analysis and X-ray imaging were carried out using an Itrax™ (Cox Analytical Systems) X-ray fluorescence (XRF) core scanner (Institute of Geological Sciences, University of Bern), equipped with a Molybdenum tube (50 keV, 30 mA) with a 10 s count-time using sampling steps of 1 mm (XRF) and 0.2 mm (X-ray imaging). Several studies could demonstrate that counts received from XRF core scanning are proportional to element concentrations if no important matrix effects due to pronounced lithology changes or variations of pore water volume and chemical composition are present (e.g. Kylander et al., 2013; Russell et al., 2014). Geochemical data were applied to identify event layers at high resolution through their higher content in detrital material (e.g. Arnaud et al., 2012; Wilhelm et al., 2012b; Czymzik et al., 2013; Swierczynski et al., 2013) and/or as high-resolution grain-size analysis (e.g. Cuven et al., 2010; Wilhelm et al., 2012a, 2013). Geochemical analyses were carried out on core FOR13P2. X-ray images highlighting the variability of the sediment density have been acquired for the four cores.

Grain size analyses on core FOR13P2 were performed using a Malvern Mastersizer 2000 (Institute of Geography, University of Bern) on sub-samples collected at a 5 mm continuous interval. Before grain-size analysis, the samples were treated in a bath of diluted (30 %) hydrogen peroxide during 3 days to remove organic matter. The disappearance of the organic matter was checked through smear slides observations. These grain-size analyses of the detrital material were performed to characterize event layers and, when event layers are induced by floods, to establish a proxy of flood intensity. Grain-size variability is assumed to be related with the stream flow energy of the river entering the lake and, thereby, with the peak discharge reached during the flood event (Campbell, 1998; Lapointe et al., 2012; Wilhelm et al., 2015). The flood intensity may also be reconstructed based on the amount of sediment transported and deposited during floods (e.g. Schiefer et al., 2011; Jenny et al., 2014; Wilhelm et al., 2015). This approach appears particularly relevant in case of an insignificant variability of the flood-sediment grain size (e.g. Jenny et al., 2014; Wilhelm et al., 2015). When the depositional pattern of the flood layers within the lake basin (assessed through the stratigraphic correlation) shows a high variability, many cores are required for a reliable assessment of the flood-sediment volumes (e.g. Page et al., 1994; Schiefer et al., 2011; Jenny et al., 2014). However, when the depositional pattern of the flood layers is stable over time, the layer thickness in one core may be sufficient (e.g. Wilhelm et al., 2012b, 2015). As a result, grain size and sediment volume of the event layers were both explored as two distinct proxies of flood intensity.

3.3 Coprophilous fungal spores analysis

Erosion processes in high-altitude catchments may be modified by grazing activity and, thereby, the climatic signal in flood reconstructions may be altered (e.g. Giguet-Covex et al., 2012). The variability of grazing intensity in a catchment area can be reconstructed from the sedimentary abundance of coprophilous fungal ascospores, i.e. *Sporormiella* (HdV-113) (e.g. Davis and Schafer, 2006; Etienne et al., 2013). To test the potential impact of grazing intensity on the reconstructed flood activity, *Sporormiella* abundance was determined in subsamples collected all along the core FOR13P3 with an approximate step of 3 cm. This core was chosen because it was the sequence with the thinnest potentially erosive event layers. During the sampling, event layers were avoided because they may correspond to layers induced by flood or mass-movement events that may have transported unusual quantities of *Sporormiella* ascospores, or induced the remobilization of older sediments. Subsamples were chemically prepared according to the procedure of Fægri and Iversen (1989). *Lycopodium clavatum* tablets were added in each subsample (Stockmarr, 1971) to express the results in concentrations (number cm^{-3}) and accumulation rates (number $cm^2\,yr^{-1}$). Coprophilous fungal ascospores were identified based on several catalogues (Van Geel and Aptroot, 2006; Van Geel et al., 2003) and counted following the procedure established by Etienne and Jouffroy-Bapicot (2014).

3.4 Dating methods

For dating the lake sequence over the last century, short-lived radionuclides (^{210}Pb, ^{137}Cs) were measured by gamma spectrometry at the EAWAG (Zürich, Switzerland). The core FOR13P4 was sampled following a non-regular step of 1 ± 0.2 cm. The non-regular step aims at matching the facies (i.e. sedimentary background or event layer) boundaries for homogeneous samples. The ^{137}Cs measurements allowed two main chronostratigraphic markers to be located: the fallout of ^{137}Cs from atmospheric nuclear weapon tests culminating in AD 1963 and the fallout of ^{137}Cs from the Chernobyl accident in AD 1986 (Appleby, 1991). The decrease in excess ^{210}Pb and the Constant Flux/Constant Sedimentation (CFCS) allowed a mean sedimentation rate to be calculated (Goldberg, 1963). The standard error of the linear regression of the CFCS model was used to estimate the uncertainty of the sedimentation rate obtained by this method. The ^{137}Cs chronostratigraphic markers are then used to control the validity of the ^{210}Pb-based sedimentation rate.

To date the sequence beyond the last century, small-size vegetal macro-remains were sampled in core FOR13P4. Terrestrial plant remains were isolated at the Institute of Plant Sciences (University of Bern) and sent for AMS ^{14}C analysis to the AMS LARA Laboratory (University of Bern). ^{14}C ages were calibrated using the Intcal13 calibration curve (Reimer et al., 2013; Table 1). In addition, palaeomagnetic chronos-

tratigraphic markers were also used. These markers can be obtained by comparing the characteristic declination and inclination of remanent magnetization (ChRM) versus depth to global geomagnetic models or to known secular variations of the geomagnetic field (e.g. Barletta et al., 2010; Wilhelm et al., 2012a). Palaeomagnetic investigations were performed at the CEREGE laboratory (University Aix-Marseille) and are detailed in Supplement.

Using the R-code package "clam" (Blaauw, 2010), an age-depth model was generated from the ^{210}Pb ages, the ^{14}C ages and the palaeomagnetic chronological markers.

4 Results

4.1 Sedimentology

The sediment consists of a homogeneous, brown mud mainly composed of silty detrital material and aquatic organic remains (small fragments of plants and anamorphous organic matter), representing the background hemi-pelagic sedimentation. These fine grained deposits are interrupted by 171 rather coarser-grained layers, which are interpreted to represent short-term depositional events, i.e. event layers (Fig. 2).

The 171 event layers correspond to graded layers, characterized by their higher density, a slight fining-upward trend and a thin, whitish fine-grained capping layer (Fig. 2). There is no evidence of an erosive base. According to the stratigraphic correlation, almost all these graded layers (168 out of 171) extend over the entire lake basin with a regular deposition pattern. The thickness of these 168 graded layers is systematically larger in cores FOR13P2 and FOR13P4, and decreases, respectively in cores FOR13P1 and FOR13P3. This suggests that the southern branch of the Bouchouse stream is the main sediment input over the studied period (Fig. 1). The grain-size of these graded layers is dominated by silt-sized grains with only small amounts of clay and/or fine silt present in the whitish capping layer and to coarse silt in their basal part (Figs. 2 and S1 in Supplement). The origin of these 168 is discussed in Sect. 5.1. The three other graded layers show a higher variability in thickness, grain size and depositional pattern. Above all, they overlie 3 cm coarse-grained layers, present at 75 cm in core FOR13P2 and at 9 and 42 cm in core FOR13P4 (Fig. 2). The coarse-grained layers consist of pebble gravels and aquatic plant remains embedded in a silty matrix. The high porosity in the sediment due to the presence of gravels generates a partial loss of XRF signal, preventing a reliable geochemical characterization. X-ray images show chaotic sedimentary structures. The stratigraphic correlation revealed that 2 cm of sediment are missing below the thickest coarse-grained layer in core FOR13P4, suggesting an erosive base for this layer. The stratigraphic succession of a coarse-grained layer overlain by a graded layer (labelled MMIL in Figs. 2 and 3) suggests that the two layers were induced by a single event. Their origin is discussed in Sect. 5.1.

4.2 Geochemistry

Among the core scanner output parameters, the scattered incoherent (Compton) radiation of the X-ray tube (Mo_{inc}) may vary with the sediment density (Croudace et al., 2006) and, thereby, offer a high-resolution proxy for sediment density. Mo_{inc} values were averaged at a 5 mm resolution to be compared to the density obtained at a 5 mm resolution with the gamma-ray attenuation method. A positive and significant correlation ($r = 0.85$, $p < 10^{-4}$) between the two density parameters was found and allowed using Mo_{inc} as a proxy of sediment density for identifying millimetre-scale event layers (Fig. 3).

The variability of other elements within the event layers was then investigated to assess (i) a high-resolution grain-size proxy and (ii) distinct sediment sources of the event layers between the littoral (i.e. mass-movement origin) and the catchment area (i.e. flood origin). The variability of potassium (K) intensities vs. sediment depth (Figs. 2 and S1) shows increased K intensities in the capping layers of the event layers, suggesting K enrichment in the finest sediment fraction. Variability in silicon (Si) intensities is correlated to K intensities ($r = 0.77$, $p < 10^{-4}$). Variations in iron (Fe) intensities show an opposite pattern with Fe enrichments in the basal and coarser part of the graded beds. Interestingly, Fe is the only element which elevated in event layers. These results suggest that the Fe / K ratio may be used as a millimetre-scale proxy for relative grain-size distribution and hence for detecting millimetre-scale event layers. However, since grain-size variability is insignificant, the information that can be won from this proxy in regard to flood-intensity reconstruction is minor.

Ca intensities are most of the time very low (< 900 counts), except for several sharp peaks and two well-marked excursions (> 1200 counts) at 30 and 75 cm in core FOR13P2 (Fig. 3). These two well-marked excursions correspond to the two thickest graded layers (labelled MMIL2 and 3; Fig. 2). In addition, manganese (Mn) intensities also vary within a low value range (< 10^4 counts) interrupted by sharp, well-marked peaks (up to 4.10^4 counts). All those Mn peaks are located at the base of the 168 graded layers (those that not overlain a coarse-grain layers). However not every base of graded layers corresponds to a Mn peak. To better assess the relationships between those elements, the Ca intensities were plotted against Fe, K and Mn intensities (Fig. 3). These plots clearly highlight two groups of deposits. The background sediments and the 168 graded layers (those labelled FIL in Fig. 3) are characterized by (i) low Ca intensities and (ii) a high variability in Mn intensities. The three graded layers labelled MMIL in Fig. 2 show a distinct geochemical pattern with (i) high Ca intensities regardless of Fe and K intensities and (ii) very low Mn intensities.

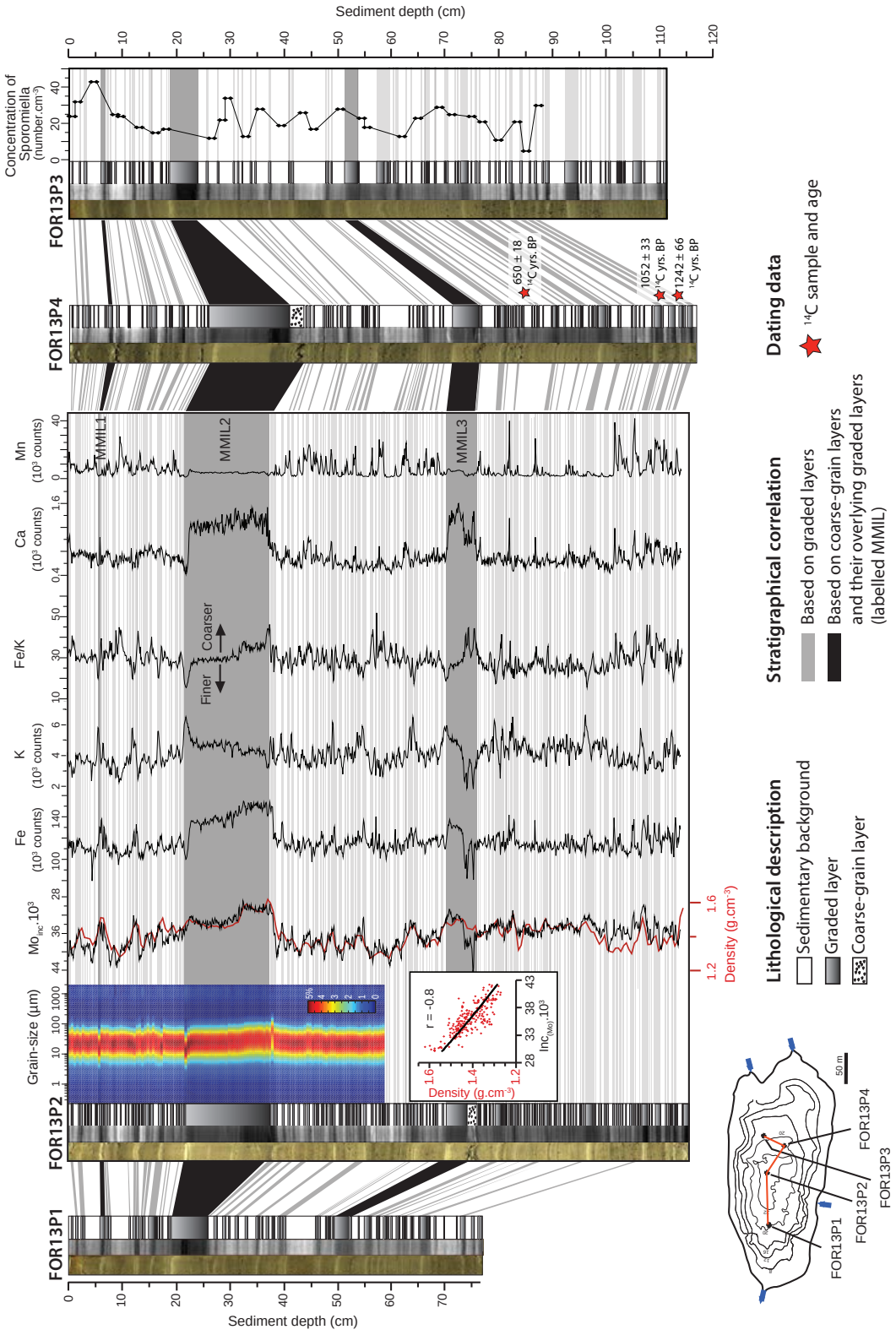

Figure 2. Lithological descriptions of cores and stratigraphic correlations based on sedimentary facies. For each core, a photo (left), an X-ray image (centre) and a stratigraphic log is shown (right). ^{14}C samples are indicated by red stars. Variability in grain-size distribution and geochemical elements (Fe, K, Ca and Mn) is shown for the core FOR13P2. Mo_{inc} used as a high-resolution proxy of density is shown close to the density measurements performed by gamma-ray attenuation. Variability in Sporomiella concentration is shown for core FOR13P3.

Table 1. Radiocarbon dates of core FOR13P4. We calculated the event-free sedimentary depth by removing the graded beds, which were considered to be instantaneous deposits. See text for explanation, nature of samples and calibration procedures.

BE nr.	Core	Core depth (cm)	Core depth in core FOR13P2 (cm)	Event-free depth in core FOR13P2 (cm)	Material	14C yrs. BP	Cal. yrs BP ($\pm 2\sigma$)	Cal. yrs AD ($\pm 2\sigma$)
2094.1.1	FOR13P4	84–85	82–83	33	Terrestrial	650 ± 18	561–665	1285–1389
2095.1.1	FOR13P4	109–111	106–108	46 ± 0.5	plant	1052 ± 33	923–1052	898–1027
2096.1.1	FOR13P4	113–115	110–112	47 ± 0.5	remains	1242 ± 66	1004–1292	658–946

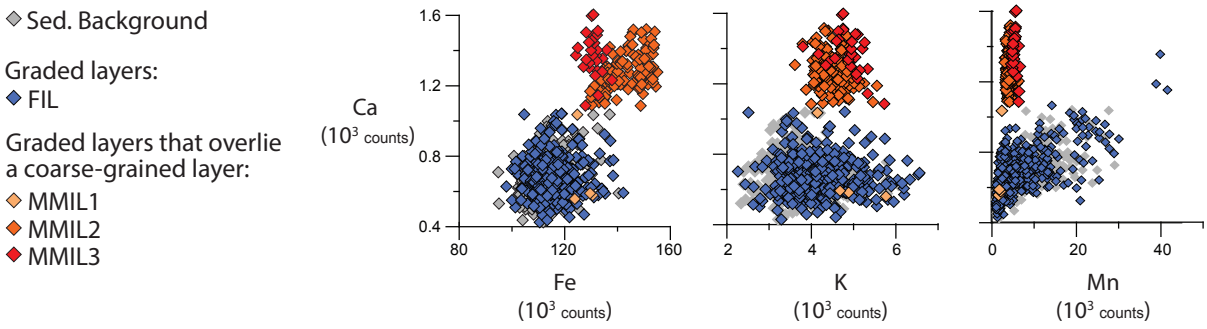

Figure 3. To illustrate the different geochemical characteristics of the sedimentary background and the graded layers, their Ca intensities were plotted against their Fe, K and Mn intensities. FIL refers to flood- and MMIL to mass-movement-induced layers. The different MMILs are labelled according to Fig. 2.

4.3 Chronology

The down-core ^{210}Pb excess profile for core FOR13P2 shows a continuous decrease to low values ($\sim 50\,\mathrm{Bq\,Kg^{-1}}$), punctuated by sharp excursions to low values for three layers (2–3.5, 7.5–10.5 and 15–17 cm) corresponding to graded layers (Fig. 4a). In line with Arnaud et al. (2002), these values were excluded to build a corrected sedimentary record without event layers (Fig. 4b). The CFCS model (Goldberg, 1963), applied on the event-free ^{210}Pb excess profile, provides a mean sedimentation rate of $1.3 \pm 0.1\,\mathrm{mm\,yr^{-1}}$ (without the event layers). Ages derived from the CFCS model were transposed to the original sediment sequence to provide a continuous age–depth relationship (Fig. 4c). The event-free ^{137}Cs profile indicated two peaks at 3.5 and 5.5 cm (Fig. 4b), interpreted as the result of the Chernobyl accident in AD 1986 and the maximum fallout of the nuclear weapon tests in AD 1963. These independent chronological markers are in good agreement with the ^{210}Pb excess ages, supporting the age-depth model over the last century (Fig. 4c).

In order to evaluate the reliability and efficiency of the palaeomagnetic results several points need to be verified: (i) the preservation of the sedimentary magnetic fabric, (ii) the stability of magnetic mineralogy, and (iii) the stability of the magnetic components. Results of Anisotropy of Magnetic Susceptibility for core FOR13P4 show a well preserved sedimentary fabric, i.e. Kmin inclination close to the vertical, except in the thickest event layers (labelled MMIL2 and MMIL3, Fig. 2) where the Kmin inclination is clearly deviated (Fig. S2). For the three cores, the mean destructive field of ARM and IRM is very similar (between 20 and 30 mT) indicating a magnetic mineralogy mainly composed of low coercivity phase. The *S* ratio (Bloemendal et al., 1992) is always between 0.86 and 0.95 indicating lower coercivity and a ferrimagnetic mineralogy. This suggests a good stability of the magnetic mineralogy, except in event layers where other parameters such as the relative palaeointensity (calculated as NRM intensity divided by ARM intensity) are clearly different, highlighting a different magnetic mineralogy. PCA have then been performed using puffin plot software (Lurcock and Wilson, 2012) to calculate the ChRM. A careful examination of demagnetization diagrams shows a unidirectional behaviour (Fig. S3). The mean angular deviation (MAD) is usually lower than 6 revealing a good stability of the magnetization direction. In most cases, the calculated component is not straight to the origin. This is particularly the case in the event layers. This implies the occurrence of a high coercivity component of unknown origin. All cores show quite large variations of the declination and inclination vs. depth. Because of the deviation of the Kmin and changes in magnetic mineralogy, measurements from the thickest event layers (i.e. MMIT2 and MMIT3) have been removed to build event-free declination and inclination signals (Fig. 5a). Based on the stratigraphic correlation, the event-free palaeomagnetic profiles obtained for each core were all corrected to a reference depth, i.e. the event-free depth of core FOR13P2 (Fig. 5b). Finally, all magnetic profiles were averaged to obtain unique curves of declination vs. depth and inclination vs. depth (Fig. 5c), smoothing small artefacts and making it easier for comparison to the reference curve (ARCH3.4k model;

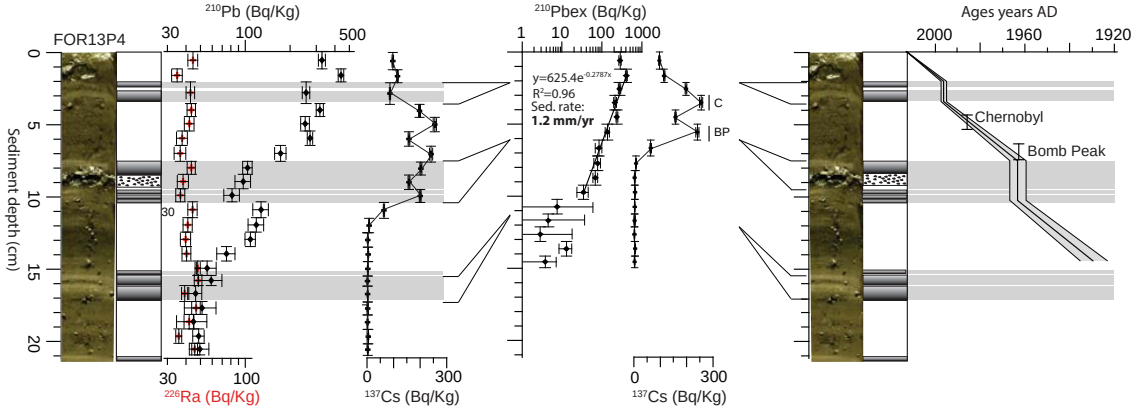

Figure 4. **(a)** ^{226}Ra, ^{210}Pb and ^{137}Cs profiles for core ALO09P12. **(b)** Application of a CFCS model to the event-free sedimentary profile of ^{210}Pb in excess (without the thick graded beds considered as instantaneous deposits). **(c)** Resulting age–depth relationship with 1σ uncertainties and locations of the historic ^{137}Cs peaks supporting the ^{210}Pb-based ages. C corresponds to the historic ^{137}Cs peak of Chernobyl (AD 1986) and MP to the maximum ^{137}Cs peak of the nuclear fallout (AD 1963).

Donadini et al., 2009; Korte et al., 2009). From the variations of the reference curve over the last millennium, magnetic declination minima and maxima can be identified at AD 1810 ± 20, 1540 ± 70 and 1365 ± 25 (D-1 to D-3, respectively). For the inclination, two tie points at AD 1700 ± 30 and 1330 ± 40 can be used (I-1 and I-2, Fig. 5d). Furthermore the ChRM declination profile presents 3 declination features and the ChRM inclination profile presents 2 inclination features over this period, allowing the correlation proposed (Fig. 5). These well-correlated declination and inclination features can thus be used as additional chronological markers.

The ^{210}Pb and the ^{14}C ages (Fig. 4 and Table 1) were then combined with the palaeomagnetic chronomarkers (Fig. 5) to construct an age-depth model covering the whole sequence (Fig. 6). As noted above, the age-depth model was calculated on an event-free depth using a smooth spline with the "clam" R-code package (Blaauw, 2010). This revealed that the sequence FOR covers the last millennium with a mean sedimentation rate of 1 mm yr^{-1} (without event layers).

5 Discussion

5.1 Different triggers for event layers

5.1.1 Mass movements

The unusual presence of gravel and aquatic plant remains, in combination with the chaotic sedimentary structures and the localized deposition areas, suggests that the coarse-grained layers result from a mass movement originating from sediment-charged slopes (e.g. Sauerbrey et al., 2013). The three graded layers overlying the coarse-grained layers then result from the sediment that is transported in suspension during sliding of subaquatic slope sediments and then deposited over the coarse-grained layers and further into the lake basin (e.g. Girardclos et al., 2007; Moernaut et al., 2014). As a result, each stratigraphic succession of a graded and a coarse-grained layer is interpreted as a mass-movement-induced layer (MMIL). These MMILs are well characterized by higher Ca intensities that suggest a distinctly different sediment source when compared to the sedimentary background and to the 168 graded layers that do not overlie a coarse-grain layer. The coarse-grained layer of MMIL3 is only present in core FOR13P3, suggesting a littoral origin of the mass movement (Fig. 2). The two coarse-grained layers of MMIL1 and MMIL2 are located in core FOR13P4 (Fig. 2). These layers may thus originate either from the delta or from the littoral slopes. Slope angles of $< 10°$ and $\sim 15°$ for delta and littoral slopes of Lake Foréant, respectively, point to a littoral origin as suggested by many studies showing that slope angles $> 10°$ are favourable for the generation of mass-movements (e.g. Moernaut et al., 2007; Strasser et al., 2011; Van Daele et al., 2013). In addition, higher Ca intensities are often an indicator of littoral sediments as a result of increased fluxes of endogenic calcite when compared to the open-water endogenic production.

5.1.2 Flood events

The 168 graded layers may be induced by either mass movements or flood events (e.g. Sturm and Matter, 1978). Their extents over the whole basin with a relatively homogeneous deposition pattern, their frequent occurrence and a different geochemical pattern suggest a distinct origin from that of the MMIL graded layers. The low Ca intensities suggest a minor sediment contribution of the marble and calc-schists in favour of a major contribution of the arkose band, which is the lithology drained by the main inflow (Fig. 1). The 168 graded layers are also characterized by sharp peaks of Mn only located at their bases. This location suggests that the

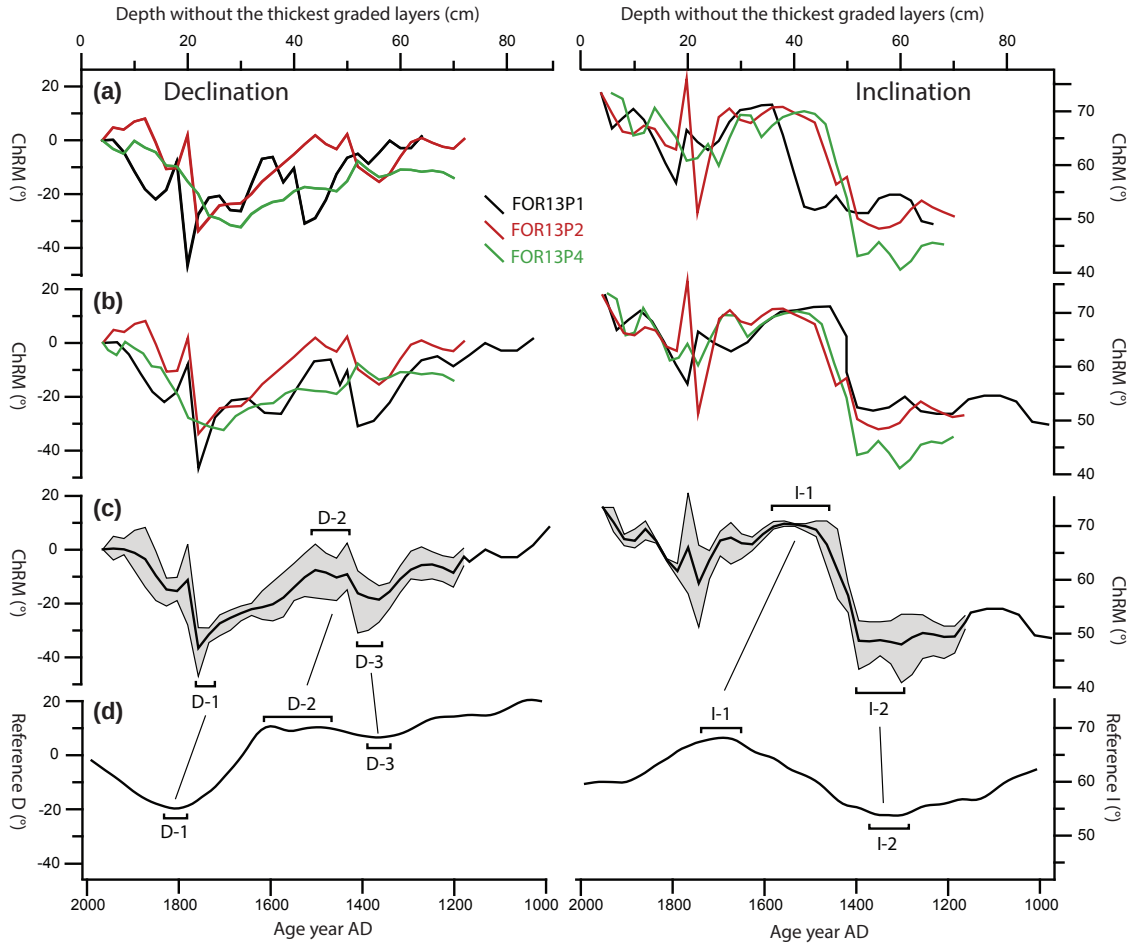

Figure 5. **(a)** Raw declination and inclination profiles of cores FOR13P1, FOR13P2 and FOR13P4. **(b)** The same profiles after removal of the thickest graded beds (interpreted as event layers) and adjustment of the different specific-core depths to a common reference depth. **(c)** Average of profiles shown in **(b)**. **(d)** Correlation to the ARCH3.4k model reference curve of declination and inclination (Donadini et al., 2009; Korte et al., 2009). ChRM means characteristic remanent magnetization. The well-correlated declination and inclination features are labelled D-x and I-x, respectively.

punctual enrichment in Mn is related to the occurrence of these event layers. Mn is a redox sensitive element and more soluble under reducing conditions (e.g. Davison, 1993; Torres et al., 2014). The punctual presence of detectable Mn at the base of the graded layers suggests that hyperpycnal turbidity currents carry oxygen to the deeper parts of the basin. Dissolved oxygen is probably also trapped in pore waters of the individual graded layers. Based on these considerations we suggest that dissolved and reduced Mn is, in part due to the rapid increase in loading from the graded layers, migrating from pore waters of the buried sediments into oxygenated graded layers where it is oxidized and precipitated likely in the form of an Mn-oxyhydroxide (e.g. Davison, 1993; Deflandre et al., 2002). The fast sediment deposition during the event-layer formation and the low reactive organic matter concentrations would then prevent reductive dissolution of the Mn-oxyhydroxide precipitates (e.g. Torres et al., 2014).

According to these layer characteristics, flood events are the most probable candidate to trigger the 168 graded layers because (i) these events may be frequent (e.g. Czymzik et al., 2013), (ii) these events may bring both high oxygen and detrital inputs in a short time (e.g. Deflandre et al., 2002), and (iii) the nature of the sediment corresponds the most to the main lithology drained by the inflow. Hence, the 168 graded layers likely correspond to flood-induced layers (FIL).

5.1.3 Chronological controls

MMILs can be triggered by spontaneous failures due to overloading and/or oversteepening of sediments-charged slopes, snow avalanches, rockfalls, earthquakes or fluctuations in lake levels (e.g. Monecke et al., 2004; Girardclos et al., 2007; Moernaut et al., 2014). In case of Lake Foréant, changes in lake level can be excluded because water levels of Lake

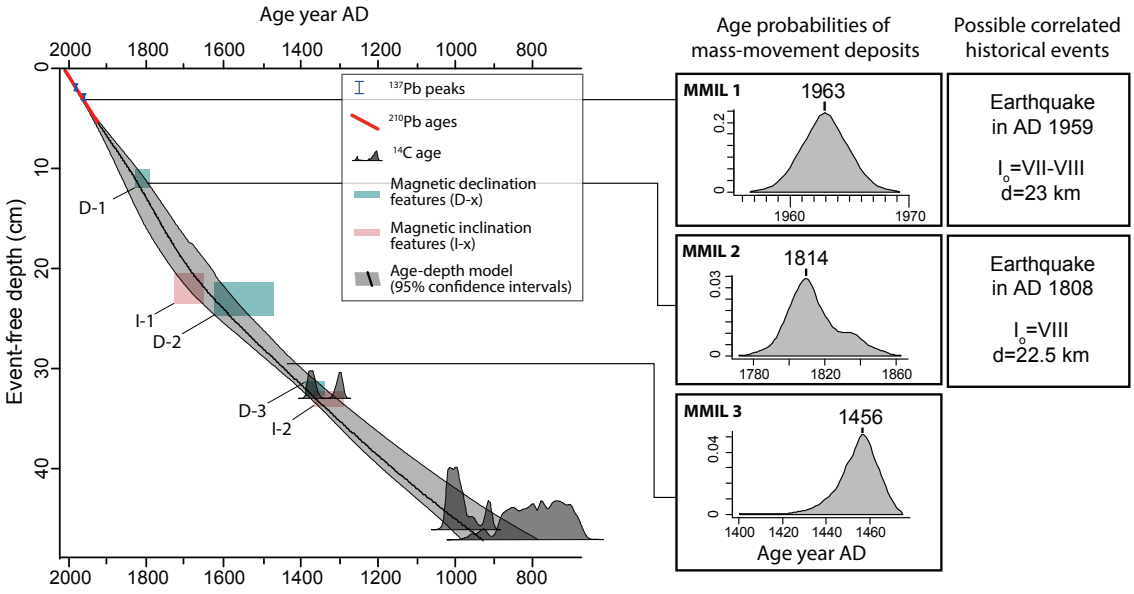

Figure 6. Age–depth model for core FOR13P2 calculated using the "clam" R-code package, combining historic ^{137}Cs peaks, ^{210}Pb ages, calibrated ^{14}C ages and magnetic features on the left side. Probability distribution frequencies of mass-movement ages and possible correlations to historical earthquakes on the right side.

Foréant are well controlled by bedrock outlets. In addition, there is no geomorphological evidence of major rockfalls in the catchment area. Regarding earthquakes, many events occurred in the region and affected the population and infrastructure. Historical earthquakes are well documented thanks to the database SisFrance (http://www.sisfrance.net, Lambert and Levret-Albaret, 1996; Scotti et al., 2004). An earthquake trigger for the MMILs can then be investigated by comparing ages of the MMILs to the dates of the closest and/or strongest historical earthquakes (e.g. Avşar et al., 2014; Howarth et al., 2014). The three MMILs are, respectively dated to AD 1963 (±6), AD 1814 (+50/−39) and AD 1456 (+19/−56) (Fig. 6). The age of the most recent deposit is consistent with the Saint-Paul-sur-Ubaye earthquake (AD 1959), characterized by an epicentre at ca. 20 km from the lake where the MSK intensity reached VII-VIII. The age of the second deposit is consistent with the Piemont (Torre Pellice) earthquake (AD 1808), characterized by an epicentre at ca. 20 km from the lake and an MSK intensity of VIII (Fig. 6). For the older period of the third deposit, data of documented earthquakes are sparser in the catalogue, precluding a reliable assignment. The earthquakes of Saint-Paul-sur-Ubaye and Piemont are both the closest and strongest historically-known earthquakes around the lake, suggesting that they are the most probable trigger of the temporarily corresponding subaquatic landslides. Overall, there is a good agreement between major historical events and the calculated ages of the MMILs supporting their sedimentologic interpretation and the chronology over the last centuries.

5.2 Palaeoflood record

A flood chronicle of the Bouchouse stream was built by dating the 168 FILs over the last millennium. Changes in flood frequency are highlighted through a running sum of flood occurrences with an 11-year (Fig. 7) or 31-year window (Fig. 8). The absence of significant grain-size variability precludes the use of grain size to assess changes in flood intensity (e.g. Giguet-Covex et al., 2012; Lapointe et al. 2012; Wilhelm et al., 2013, 2015). The relatively homogeneous grain size of the FILs makes the sediment accumulation per event a more suitable proxy of flood intensity (e.g. Jenny et al., 2014). In addition, the relatively homogeneous flood-sediment deposition pattern within the lake basin makes it possible to use the FIL thickness as a proxy of the flood-sediment accumulation as shown by previous calibration in Alpine environments (Wilhelm et al., 2012b; Jenny et al., 2014; Wilhelm et al., 2015). Hence, the FIL thickness is here assumed to represent the flood intensity, under the condition that erosion processes and availability of erodible materials in the catchment did not change significantly over time.

5.2.1 Proxy validation

To control the reliability of our reconstruction, the Foréant palaeoflood record is compared to the historical floods at Ristolas located around 8 km downstream of the lake (Fig. 1c and Supplement). The almost absence of documented flood event for the Bouchouse stream (outlet of Lake Foréant) precludes an event-to-event comparison as undertaken with the Lake Allos record (Wilhelm et al., 2015). Hence, the 21

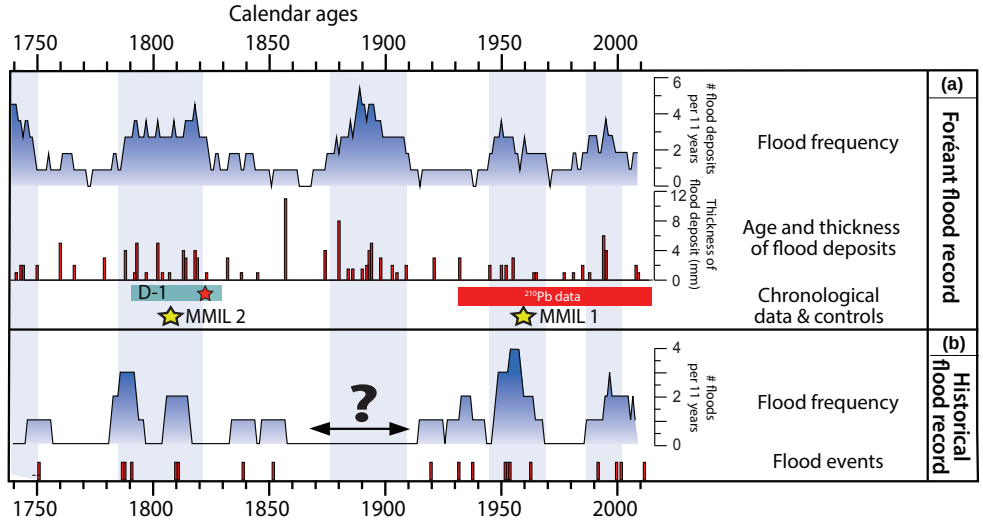

Figure 7. Comparison over the last 250 years of the reconstructed Foréant flood frequency (11-yr running sum) and intensity (thickness of flood deposits) with the frequency (11-yr running sum) of historical floods at Ristolas. The question mark refers to a possible gap in the historical data.

flood events having affected the village of Ristolas and occurring during the ice-free season of the lake (mid-June to mid-November) have been considered to reconstruct a historical flood record (Fig. 7). This includes six floods considered as "local" because they only affected the village of Ristolas (catchment area of ca. 80 km^2) and 15 floods considered as "sub-regional" because they also affected other villages downstream (Abriès, Aiguilles, Chateau-Vieille-Ville, catchment area of $\sim 320\,km^2$). Through comparison of the historical chronicles and the lake records, we observe that the ranges of flood-frequency values are similar, i.e. between 0 and around 4 floods per 11 years. We also observe strong similarities in the two flood records with common periods of low flood frequency in AD 1750–1785, 1820–1860 and 1910–1945 and common periods of high flood frequency in AD 1785–1820, AD 1945–1970 and AD 1985–2000. Only a slight time lag (~ 5 years) appears for the latter period in the lake record. Overall, there is then good agreement with the historical data, supporting that Lake Foréant sediments record the variability of past flood events that impacted societies over the last 250 years relatively well. A major inconsistency, however, appears from 1860 to 1910 since numerous floods are documented in the lake record but there is missing evidence for flood in the historical record. A high hydrological activity is documented for the region at this time (e.g. Miramont et al., 1998; Sivan et al., 2010; Wilhelm et al., 2012a, 2015), suggesting that this may result in a historical database which is locally incomplete.

5.2.2 Potential influences of environmental changes

The Foréant flood record may be considered as relevant over the entire studied period if erosion processes are stable over time. Erosion processes in the Foréant catchment may be affected by modifications in the river system and/or by land-use changes.

The main inflow, the Bouchouse stream, has built an alluvial plain upstream of the lake where it is divided in two main meandering branches. An alternate activity of these branches during floods may disturb the flood record by triggering variable sediment dispersion within the lake basin (e.g. Wilhelm et al., 2015). However, such processes seem to be unlikely because the stratigraphic correlation highlights a stable pattern of the flood-sediment deposition with the thickest FILs in cores FOR13P2 and FOR13P4 from the depocenter and a thinning of the FIL deposits toward cores FOR13P1 and FOR13P3 located in the slopes (Fig. 2). The alluvial plain may also disturb the record by acting as a sediment trap. Indeed, the meandering river morphology and the gentle slope of the alluvial plain may trigger a decrease of the discharge velocity, resulting in the deposition of the coarser particles on the plain before entering the lake. This may explain the small variability in grain-size in the Foréant sediment record. The grain-size ratio between the base (coarser fraction) and the top (finer fraction) of the FILs is ~ 1.3, while it usually ranges from 5 to 15 in many different geological and environmental settings (e.g. Oslegger et al., 2009; Giguet-Covex et al., 2012; Simmoneau et al., 2013; Wilhelm et al., 2013 Amman et al., 2015; Wilhelm et al., 2015). However, fine particles (i.e. clays and fine silts that composed the FILs) are transported by suspension in the river (e.g. Passega, 1964). As a result, their trapping and storage in the alluvial plain is unlikely. A negligible storage effect on the fine fraction is also supported by the relatively stable sedimentation rate of the silty sedimentary background (Fig. 6) that suggests an

uninterrupted sediment transport to the lake over the studied period.

Erosion processes in the catchment may also be modified by land-use that mainly corresponds at this altitude to changes in grazing intensity. An increase of grazing intensity may make soils more vulnerable to erosion during heavy rainfalls and, thereby, may induce an increased sensitivity of the catchment-lake system to record floods, i.e. higher flood frequency and/or flood-sediment accumulation in the sediment record (e.g. Giguet-Covex et al., 2012). Abundance of *Sporormiella* is assumed to reflect local changes of grazing intensity in Lake Foréant catchment (e.g. Etienne et al., 2013). The concentration of *Sporormiella* ascospores measured in core FOR13P3 oscillated from 5 to 43 number cm^{-3} through the sequence (Fig. 2), resulting in accumulation rates varying from 12 to 340 number $cm^2\ yr^{-1}$ over time (Fig. 8). This variability in *Sporormiella* abundance has been compared to the variability in flood frequency and flood-sediment accumulation (see Supplementary Material). We do not find significant relationships ($p > 0.05$) between these parameters (Fig. S4), suggesting that variations in pastoralism seemingly have not had a significant impact on erosion processes in the Foréant catchment. However, two samples covering the period AD 1734–1760 show both high *Sporormiella* accumulation rates and flood frequencies (Figs. 8 and S3). This suggests that the flood frequency during this period may be exacerbated by a punctual and very high grazing intensity. Hence, we postulate that erosion processes did not change drastically over the studied period, implying that climate is likely the main factor explaining the recorded flood activity, with the exception of the period AD 1734–1760.

5.2.3 Palaeoflood activity in the regional climatic setting

Comparison with the historical record shows that the past flood variability is well reproduced by the Foréant record (Fig. 7). The Foréant palaeoflood record is thus interpreted as the recurrence of summer-to-autumn flood events triggered by both local and mesoscale convective phenomena.

To discuss the millennium-long flood variability in regard to both Atlantic and Mediterranean climatic influences in the Alpine domain, the Foréant palaeoflood record is compared to the palaeoflood records of Lakes Blanc and Allos (Figs. 7 and 8). Lakes Blanc and Allos have similar characteristics to Lake Foréant such as the high altitude (> 2000 m a.s.l.), the small catchment area (< 3 km^2) and the steep catchment slopes, making the comparison possible. Lake Blanc sediments located in the northern French Alps mainly record Atlantic-sourced weather pattern of high altitude, i.e. summer local convective events (Fig. 1; Giguet-Covex et al., 2012; Wilhelm et al., 2012b, 2013). In contrast, Lake Allos sediments located in the southern French Alps mainly record Mediterranean-sourced weather patterns of high altitude, i.e. mesoscale convective events (Fig. 1; Wilhelm et al., 2012a, 2015). The last millennium is usually divided in three climatic periods according to the temperature variations; the warm Medieval Climate Anomaly (MCA, ca. AD 950–1250), the cold Little Ice Age (LIA, ca. AD 1300–1900) and the warmer 20th century (e.g. Lamb, 1965; Büntgen et al., 2011; Luterbacher et al., 2012 and references therein). During the MCA, the Foréant flood record shows a low flood frequency with ∼ 10 floods per century and, 4 occurrences of thick flood deposits (> 8 mm thick) that we interpret as high-intensity flood events. During the LIA, the Foréant record shows a higher flood frequency with ∼ 17 floods per century and only 2 high-intensity events. The 20th century is finally characterized by ∼ 17 floods per century and an absence of high-intensity events. The increased flood frequency during the long and cold period of the LIA, compared to the MCA, was also observed in the Blanc and Allos records (Wilhelm et al., 2012a, 2013; Fig. 8), as well as in many other records from the European Alps (e.g. Arnaud et al., 2012; Glur et al., 2013; Swierczynski et al., 2013; Wirth et al., 2013a, b; Amann et al., 2015; Schulte et al., 2015) and the north-western Mediterranean area (e.g. Jorda and Provansal, 1996; Camuffo and Enzi, 1995; Jorda et al., 2002; Thorndycraft and Benito, 2006; Moreno et al., 2008; Benito et al., 2015; Arnaud-Fassetta et al., 2010). This common pattern in many flood records of southern Europe may be the result of a southward shift and an intensification of the dominant westerly winds during boreal summer related to an increase in the thermal gradient between low (warming) and high (cooling) latitudes (e.g. Bengtsson and Hodges, 2006; Raible et al., 2007). In this scenario, the Alps are likely to experience an increase in precipitation due to an increase in moisture advection from the North Atlantic. In contrary, the occurrence of high-intensity floods during both the MCA and the LIA periods is a new feature of Alpine regional patterns, since the most intense floods occurred exclusively during the MCA in the Blanc record (Wilhelm et al., 2013) or during the LIA in the Allos record (Wilhelm et al., 2012a; Fig. 8) and other Mediterranean records of the Alpine region (Jorda and Provansal, 1996; Miramont et al., 1998; Jorda et al., 2002; Arnaud-Fassetta et al., 2010). This suggests that hydro-meteorological processes related to the Atlantic and to the Mediterranean climatic influences may alternatively trigger high- intensity events in the Foréant area during the MCA and the LIA, respectively. However, the most intense floods at Foréant appear 3 times more frequently during the MCA than during the LIA, a trend that remains true when considering various thickness thresholds (8, 7, 6 or 5 mm) for high-intensity flood events. In addition, the mean sediment accumulation per flood event shows values ∼ 50 % higher during the MCA than during the LIA (3.8 vs. 2.4 mm $flood^{-1}$), suggesting an increase of the mean flood-event intensity during the warmer period. These two evidences of increased flood intensity during the warm period may be related to the strengthening of local convective processes due to higher temperatures, as suggested for the north-western flood pattern (Giguet-Covex et al., 2012; Wilhelm et al., 2012b, 2013).

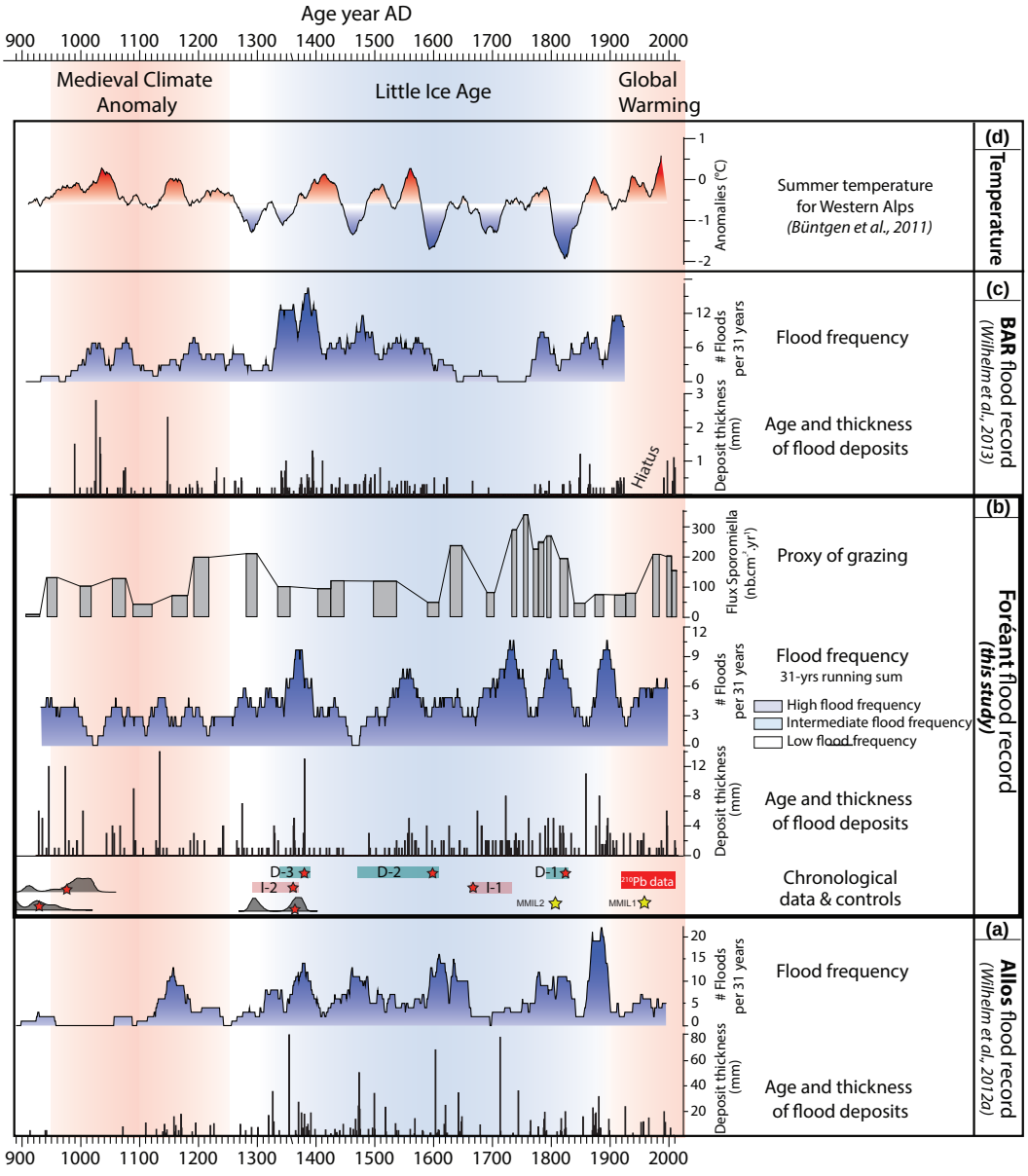

Figure 8. Comparison over the last millennium of **(b)** the reconstructed Foréant flood frequency (31-year running average) and intensity (thickness of flood deposits) with **(a)** the Allos flood record from the southern French Alps (Wilhelm et al., 2012a), **(c)** the BAR flood record from the northern French Alps (Wilhelm et al., 2013) and **(d)** the tree-ring-based summer temperature for the European Alps (Büntgen et al., 2011). The reconstructed *Sporomiella*-type flux is also shown next to the Foréant flood record to highlight potential human impacts (i.e. grazing) on the erosion processes that might bias the flood record. The red stars below the Foréant record show the chronological markers with their 2-sigma uncertainty ranges.

In the Foréant area, higher temperatures seem thus to result in a lower flood frequency but in higher flood intensity on the multi-centennial timescale. Flood frequency and intensity during the warmer 20th century, however, do not follow these trends. The frequency is still similar to the LIA one and high-intensity events are absent and the mean sediment accumulation per flood event (2.2 mm flood^{-1}) is also similar to the LIA. Two hypotheses may be considered to explain this "anomaly". First, this may result from the relatively short period covered by the 20th century (i.e. $\sim$ 100 years) in comparison with the multi-centennial variability documented for the MCA (i.e. $\sim$ 300 years) and the LIA (i.e. $\sim$ 600 years) periods. Thereby, considering stable temperature–flood relationships over time, the 20th century might be a transitional period toward an MCA-like flood pattern with the global warming. This latter possibility would imply an increasing flood

hazard in the Foréant region in the near future due to an increased occurrence of high-intensity flood events. Secondly, this may also result from a non-linearity of the flood response to temperature, making the analogy between the MCA and the 20th century more complex, in particular as the current warming is caused by an unprecedented forcing (greenhouse gases). Moreover, the other external forcing such as solar activity, and volcanic eruptions largely varied over the last millennium (e.g. Servonnat et al., 2010; Delaygue et Bard, 2011; Gao et al., 2012; Crowley and Unterman, 2013) and their non-linear combination also with the greenhouse gases may result in different time-space temperature patterns and, thereby, in different flood responses during these two periods. In order to explore forcing-dependent impacts on the climate-flood relationships, deeper analysis utilizing for example advanced statistics or simulations is required.

6 Conclusions

High-resolution sedimentological and geochemical analyses of the Lake Foréant sequence revealed 171 event layers. Three of the 171 event layers can be differentiated by characteristic geochemical features (high Ca contents and low Mn contents) and stratigraphic succession. These three event layers are interpreted as mass-movement-induced layers. The other 168 event layers show a geochemical pattern similar to the sedimentary background that mainly corresponds to detrital material sourced by the rivers. These event layers are interpreted as flood-induced layers. Only small changes in grain-size variability in the flood-induced layers precluded the use of the grain size as a flood-intensity proxy. However, the relatively homogeneous grain size and deposition pattern within the lake basin made the flood-deposit thickness a suitable proxy for the reconstruction of flood intensity.

Comparison with local historical data indicates that Foréant sediments sensitively record past flood events with variability in frequency and intensity related to both Atlantic- and Mediterranean-influenced hydro-meteorological processes, i.e. local and mesoscale convective systems occurring from late spring to autumn. As there is no evidence of major changes in erosion processes due to landscape evolution or grazing intensity (except maybe for the period AD 1734–1760), we assume that climate and not land-use changes exerts the dominant control on flood variability in the Foréant-record over the past millennium. The comparison to northern and southern flood records, i.e. to Atlantic- and Mediterranean-influenced records, highlights that the increase of flood frequency during the cold period of the LIA is a common feature of all regional flood patterns from the European Alps. The comparison also revealed that high-intensity events in the Foréant region occurred during both the cold LIA and the warm MCA periods. This specific feature of the Foréant flood record likely results from its sensitivity to both Atlantic and Mediterranean climatic influences. However, high-intensity events are more frequent and the flood intensity is higher during the warm MCA. This suggests that flood hazard may increase in the Foréant region in response to global warming. Surprisingly, the flood variability over the warm 20th century appears still similar to the flood variability of the cold LIA period. This 20th-century flood trend may be interpreted as the result of a transitional period toward an MCA-like flood pattern. This would imply an increasing flood hazard in the Foréant region in the near future due to more frequent high-intensity flood events. However, this may also result from a non-linear temperature–flood relationship. In order to better understand the underlying mechanisms deeper analyses employing advanced statistics or simulations need to be applied.

The Supplement related to this article is available online at doi:10.5194/cp-12-299-2016-supplement.

Acknowledgements. B. Wilhelm's post-doctoral fellowship (2013–2014) was supported by a grant from the AXA Research Fund. We would also like to thank Pierre Sabatier for his help with analysis of the ^{210}Pb data, Anne-Lise Develle for fruitful discussions, Petra Boltshauser-Kaltenrieder for help with identification of terrestrial-plant remains prior to ^{14}C dating and Nicolas Thouveny and François Demory for providing access to facilities at the CEREGE palaeomagnetic laboratory (Aix-Marseille University) and for fruitful discussions. The authors thank Gerardo Benito and an anonymous referee for their constructive comments.

Edited by: J. Luterbacher

References

Amann, B., Sönke, S., and Grosjean, M.: A millennial-long record of warm season precipitation and flood frequency for the Northwestern Alps inferred from varved lake sediments: implications for the future, Quaternary Sci. Rev., 115, 89–100, 2015.

Appleby, P. G., Richardson, N., and Nolan, P. J.: ^{241}Am dating of lake sediments, Hydrobiologia, 214, 35–42, 1991.

Arnaud, F., Lignier, V., Revel, M., Desmet, M., Pourchet, M., Beck, C., Charlet, F., Trentesaux, A., and Tribovillard, N.: Flood and earthquake disturbance of ^{210}Pb geochronology (Lake Anterne, North French Alps), Terra Nova, 14, 225–232, 2002.

Arnaud, F., Révillon, S., Debret, M., Revel, M., Chapron, E., Jacob, J., Giguex-Covex, C., Poulenard, J., and Magny, M.: Lake Bourget regional erosion patterns reconstruction reveals Holocene NW European Alps soil evolution and paleohydrology, Quaternary Sci. Rev., 51, 81–92, 2012.

Arnaud-Fassetta, G. and Fort, M.: Respective parts of hydroclimatic and anthropic factors in the recent eveolution (1956–2000) of the active channel of the Upper Guil, Queyras, Southern French Alps, Méditerranée, 102, 143–156, 2004.

Arnaud-Fassetta, G., Carcaud, N., Castanet, C., and Salvador, P. G.: Fluviatile palaeoenvironments in archaeological context: geographical position, methodological approach and global change – hydrological risk issues, Quatern. Int., 216, 93–117, 2010.

Avşar, U., Hubert-Ferrari, A., De Batist, M., Lepoint, G., Schmidt S., and Fagel N.: Seismically-triggered organic-rich layers in recent sediments from Göllüköy Lake (North Anatolian Fault, Turkey), Quaternary Sci. Rev., 103, 67–80, 2014.

Barletta, F., St-Onge, G., Channell, J. E. T., and Rochon, A.: Dating of Holocene western Canadian Arctic sediments by matching paleomagnetic secular variation to a geomagnetic field model, Quaternary Sci. Q. Rev., 29, 2315–2324, 2010.

Bengtsson, L. and Hodges, K. I.: Storm tracks and climate change, J. Climate, 19, 3518–3543, 2006.

Beniston, M. and Stephenson, D. B.: Extreme climatic events and their evolution under changing climatic conditions, Glob. Planet. Change, 44, 1–9, 2004.

Benito, G., Macklin, M. G., Zielhofer, C., Jones A., and Machado, M. J.: Holocene flooding and climate change in the Mediterranean, Catena, 130, 13–33, 2015.

Blaauw, M.: Methods and code for "classical" age modelling of radiocarbon sequences, Quaternary Geochronol., 5, 512–518, 2010.

Bloemendal, J., King, J. W., Hall, F. R., and Doh, S.-J.: Rock magnetism of Late Neogene and Pleistocene deep-sea sediments relationship to sediment source, diagenetic processes, and sediment lithology, J. Geophys. Res., 97: 4361–4375, 1992.

Boudevillain, B., Argence, S., Claud, C., Ducrocq, V., Joly, B., Lambert, D., Nuissier, O., Plu, M., Ricard, D., Arbogast, P., Berne, A., Chaboureau, J. P., Chapon, B., Crepin, F., Delrieu, G., Doerflinger, E., Funatsu, B. M., Kirstetter, P. E., Masson, F., Maynard, K., Richard, E., Sanchez, E., Terray, L., and Walfpersdorf, A.: Cyclogeneses et precipitations intenses en region mediterraneenne: origines et caracteristiques, La Meteorol., 66, 18–28, 2009.

Boroneant, C., Plaut, G., Giorgi, F., and Bi., X.: Extreme precipitation over the Maritime Alps and associated weather regimes simulated by a regional climate model: Present-day and future climate scenarios, Theor. Appl. Climatol., 86, 81–99, 2006.

Büntgen, U., Tegel, W., Nicolussi, K., McCormick, M., Frank, D., Trouet, V., Kaplan, J., Herzig, F., Heussner, U., Wanner, H., Luterbacher, and J., Esper, J.: 2500 years of European climate variability and human susceptibility, Science, 331, 578–582, 2011

Buzzi, A. and Foschini, L.: Mesoscale meteorological features associated with heavy precipitation in the Southern Alpine Region, Meteorol. Atmos. Phys., 72, 131–146, 2000.

Campbell, C.: Late Holocene lake sedimentology and climate change in southern Alberta, Canada, Quatern. Res., 49, 96–101, 1998.

Camuffo, D. and Enzi, S.: The analysis of two bi-millenary series: Tiber and Po River Floods, in: Climatic Variations and Forcing Mechanisms of the Last 2000 years, edited by: Jones, P. D., Bradley, R. S., and Jouzel, J., NATO ASI Series, Series I: Global Environmental Change, 41 Springer, Stuttgart, 433–450, 1995.

Corella, J. P., Benito, G., Rodriguez-Lloveras, X., Brauer, A., and Valero-Garcès, B. mL.: Annually-resolved lake record of extreme hydro-meteorological events since AD 1347 in NE Iberian Peninsula, Quaternary Sci. Rev., 93, 77–90, 2014.

Croudace, I. W., Rindby, A., and Rothwell, R. G.: ITRAX: description and evaluation of a new multi-function X-ray core scanner, in: New Techniques in Sediment Core Analysis, edited by: Rothwell, R. G., Geological Society, London, Special Publications, 367, 51–63, 2006.

Crowley, T. J. and Unterman, M. B.: Technical details concerning development of a 1200 yr proxy index for global volcanism, Earth Syst. Sci. Data, 5, 187–197, doi:10.5194/essd-5-187-2013, 2013.

Cuven, S., Francus, P., and Lamoureux, S.: Estimation of grain size variability with micro X-ray fluorescence in laminated lacustrine sediments, Cape Bounty, Canadian High Arctic, J. Paleolimnol., 44, 803–817, 2010.

Czymzik, M., Brauer, A., Dulski, P., Plessen, B., Naumann, R., von Grafenstein, U., and Scheffler, R.: Orbital and solar forcing of shifts in Mid- to Late Holocene flood intensity from varved sediments of pre-alpine Lake Ammersee (southern Germany), Quaternary Sci. Rev., 61, 96–110, 2013.

Davis, O. K. and Schafer, D.: *Sporormiella* fungal spores, a palynological means of detecting herbivore density, Palaeogeo., Palaeoclimatol., 237, 40–50, 2006.

Davison, W.: Iron and manganese in lakes, Earth-Sci. Rev., 34, 119–163, 1993

Deflandre, B., Mucci, A., Gagne, J. P., Guignard, C., and Sundby, B.: Early diagenetic processes in coastal marine sediments disturbed by a catastrophic sedimentation event, Geochim. Cosmochim. Ac., 66, 2547–2558, 2002.

Delaygue, G. and Bard, E.: An Antarctic view of Beryllium-10 and solar activity for the past millennium, Clim. Dynam., 36, 2201–2218, 2011.

Donadini, F., Korte, M., and Constable, C. G.: Geomagnetic field for 0–3 ka: 1. New data sets for global modeling, Geochem. Geophys. Geosys., 10, Q06007, doi:10.1029/2008GC002295, 2009.

Durant, Y., Laternser, M., Giraud, G., Etchevers, P., Lesaffre, B., and Merindol, L.: Reanalysis of 44 Yr of Climate in the French Alps (1958–2002): Methodology, Model Validation, Climatology, and Trends for Air Temperature and Precipitation, J. Appl. Meteorol. Climatol., 48, 429–449, 2009.

Etienne, D. and Jouffroy-Bapicot, I.: Optimal counting limit for fungal spore abundance estimation using *Sporormiella* as a case study, Veget. Hist. Archaeobot, 23, 743–749, 2014.

Etienne, D., Wilhelm, B., Sabatier, P., Reyss, J. L., and Arnaud, F.: Influence of sample location and livestock numbers on *Sporormiella* concentrations and accumulation rates in surface sediments of Lake Allos, French Alps, J. Paleolimnol., 49, 117–127, 2013.

Faegri, K. and Iversen, J.: Textbook of Pollen Analysis, John Wiley & Sons, New York, 328 pp., 1989.

Frei, C., Schöll, R., Fukutome, S., Schmidli, J., and Vidale, P. L.: Future change of precipitation extremes in Europe: Intercomparison of scenarios from regional climate models, J. Geophys. Res. Atm., 111, D06105, doi:10.1029/2005JD005965, 2006.

Gao, C., Robock, A., and Ammann, C.: Volcanic forcing of climate over the past 1500 years: An improved ice core-based index for climate models, J. Geophys. Res., 113, D23111, doi:10.1029/2008JD010239, 2008.

Giguet-Covex, C., Arnaud, F., Enters, D., Poulenard, J., Millet, L., Francus, P., David, F., Rey, P. J., Wilhelm, B., and Delannoy, J.

J.: Frequency and intensity of high altitude floods over the last 3.5 ka in NW European Alps, Quaternary Res., 77, 12–22, 2012.

Gilli, A., Anselmetti, F. S., Glur, L., and Wirth, S. B.: Lake sediments as archives of recurrence rates and intensities of past flood events, in: Dating Torrential Processes on Fans and Cones – Methods and Their Application for Hazard and Risk Assessment, edited by: Schneuwly-Bollschweiler, M., Stoffel, M., and Rudolf-Miklau, F., Adv. Glob. Change Res., 47, 225–242, 2012.

Girardclos, S., Schmidt, O. T., Sturm, M. , Ariztegui, D., Pugin A., and Anselmetti F. S.: The 1996 AD delta collapse and large turbidite in Lake Brienz, Mar. Geol., 24, 137–154, 2007.

Glur, L., Wirth, S. B., Buntgen, U., Gilli, A., Haug, G. H., Schär, C., Beer, J., and Anselmetti, F. S., Frequent floods in the European Alps coincide with cooler periods of the past 2500 years, Sci. Rep., 3, 2770, doi:10.1038/srep02770, 2013.

Goldberg, E. D.: Geochronology with 210Pb Radioactive Dating, IAEA, Vienna, 121–131, 1963

Gottardi, F., Obled, C., Gailhard, J., and Paquet, E.: Statistical reanalysis of precipitation fields based on ground network data and weather patterns: Application over French mountains, J. Hydrol., 432/433, 154–167, 2010.

Howarth, J. D., Fitzsimons, S. J., Norris, R. J., and Jacobsen, G. E.: Lake sediments record high intensity shaking that provides insight into the location and rupture length of large earthquakes on the Alpine Fault, New Zealand, Earth Planet. Sci. Lett., 403, 340–351, 2014.

IPCC: The Physical Science Basis, Contribution of Working Group I to the Fifth Assessment Report of the Intergovernmental Panel on Climate Change, edited by: Stocker, T. F., Qin, D., Plattner, G.-K., Tignor, M., Allen, S. K., Boschung, J., Nauels, A., Xia, Y., Bex, V., and Midgley, P. M., Cambridge University Press, Cambridge, United Kingdom and New York, NY, USA, 2013

Jorda, M. and Provansal, M.: Impact de l'anthropisation et du climat sur le detritisme en France du sud-est (Alpes du Sud et Provence), B. Soc. Geol. F., 167, 159–168 ,1996.

Jorda, M., Miramont, C., Rosique, T., and Sivan, O.: Evolution de l'hydrosysteme durancien (Alpes du Sud, France) depuis la fin du Pleniglaciaire superieur, in: Bravard, J.-P. and Magny, M., Les Fleuves ont une Histoire, Paleo-environnement des Rivieres et des lacs Francais depuis 15000 ans, Errance, Paris, 239–249, 2002.

Jenny, J.-P., Wilhelm, B., Arnaud, F., Sabatier, P., Giguet-Covex, C., Mélo, A., Fanget, B., Malet, E., Ployon, E., and Perga, M.E., A 4D sedimentological approach to reconstructing the flood frequency and intensity of the Rhône River (Lake Bourget, NW European Alps), J. Paleolimnol., 51, 469–483, 2014.

Kylander, M. E., Klaminder, J., Wohlfarth, B., and Löwemark, L.: Geochemical responses to paleoclimatic changes in southern Sweden since the late glacial: the Hässeldala Port lake sediment record, J. Paleolimnol., 50, 57–70, 2013.

Korte, M., Donadini, F., and Constable, C. G.: Geomagnetic field for 0–3 ka: 2. A new series of time-varying global models, Geochem. Geophys. Geosys., 10, Q06008, doi:10.1029/2008GC002297, 2009.

Lamb, H. H.: The early medieval warm epoch and its sequel, Palaeogeogr. Palaeoclimatol., 1, 13–37, 1965.

Lambert, J. and Levret-Albaret, A.: Mille ans de séismes en France. Catalogues d'épicentres, paramètres et references, Ouest-Editions, Presses Académiques, Nantes, 1996.

Lapointe, F., Francus, P., Lamoureaux, S. F., Saïd, M., and Cuven, S.: 1,750 years of large rainfall events inferred from particle size at East Lake, Cape Bounty, Melville Island, Canada, J. Paleolimnol., 48, 159–173, 2012.

Lionello, P., Abrantes, F., Congedi, L., Dulac, F., Gacic, M., Gomis, D., Goodess, C., Hoff, H., Kutiel, H., Luterbacher, J., Planton, S., Reale, M., Schröder, K., Struglia, M. V., Toreti, A., Tsimplis, M., Ulbrich, U., and Xoplaki, E.: Introduction: Mediterranean Climate: Background Information, edited by: Lionello, P., The Climate of the Mediterranean Region, From the Past to the Future, Amsterdam: Elsevier (Netherlands), XXXV–lXXX, ISBN:9780124160422, 2012.

Lurcock, P. C. and Wilson, G. S.: PuffinPlot: A versatile, user-friendly program for paleomagnetic analysis, Geochem. Geophys. Geosys., 13, Q06Z45, doi:10.1029/2012GC004098, 2012.

Luterbacher, J., García-Herrera, R., Akcer-On, S., Allan, R., Alvarez-Castro, M. C., Benito, G., Booth, J., Büntgen, U., Cagatay, N., Colombaroli, D., Davis, B., Esper, J., Felis, T., Fleitmann, D., Frank, D., Gallego, D., Garcia-Bustamante, E., Glaser, R., González-Rouco, J.F., Goosse, H., Kiefer, T., Macklin, M. G., Manning, S., Montagna, P., Newman, L., Power, M. J., Rath, V., Ribera, P., Riemann, D., Roberts, N., Sicre, M., Silenzi, S., Tinner, W., Valero-Garces, B., van der Schrier, G., Tzedakis, C., Vannière, B., Vogt, S., Wanner, H., Werner, J. P., Willett, G., Williams, M. H., Xoplaki, E., Zerefos, C. S., and Zorita, E.: A review of 2000 years of paleoclimatic evidence in the Mediterranean, in: The Climate of the Mediterranean region: from the past to the future, edited by: Lionello, P., Elsevier, Amsterdam, the Netherlands, 87–185, 2012.

Miramont, C., Jorda, M., and Pichard, G.: Évolution historique de la morphogenèse et de la dynamique fluviale d'une rivière méditerranéenne : l'exemple de la moyenne Durance (France du sud-est), Géogr. Phys. Quatern., 52, 381–392, 1998.

Moernaut, J., De Batist, M., Charlet, F., Heirman, K., Chapron, E., Pino, M., Brümmer, R., and Urrutia, R.: Giant earthquakes in South-Central Chile revealed by Holocene mass-wasting events in Lake Puyehue, Sediment. Geol., 195, 239–256, 2007.

Moernaut, J., Van Daele, M., Heirman, K., Fontijn, K., Strasser, M., Pino, M., Urrutia R., and De Batist, M.: Lacustrine turbidites as a tool for quantitative earthquake reconstruction: New evidence for a variable rupture mode in south central Chile, J. Geophys. Res. Solid Earth, 119, 1607–1633, doi:10.1002/2013JB010738, 2014.

Monecke, K., Anselmetti, F. S., Becker, A., Sturm, M., and Giardini, D.: The record of historic earthquakes in lake sediments of Central Switzerlanc, Tectonophysics, 394, 21–40, 2004.

Moreno, A., Valero-Garces, B. L., Gonzalez-Samperiz, P., and Rico, M.: Flood response to rainfall variability during the last 2000 years inferred from the Taravilla Lake record (Central Iberian Range, Spain), J. Palaeolimnol., 40, 943–961, 2008.

Noren, A. J., Bierman, P. R., Steig, E. J., Lini, A., and Southon, J.: Millennial-scale storminess variability in the northeastern United States during the Holocene epoch, Nature, 419, 821–824, 2002.

Oslegger, D. A., Heyvaert, A. C., Stoner, J. S., and Verosub, K. L.: Lacustrine turbidites as indicators of Holocene storminess and climate: Lake Tahoe, California and Nevada, J. Paleolimnol., 42, 103–122, 2009.

Page, M. J., Trustrum, N. A., and DeRose, R. C.: A high resolution record of storm-induced erosion from lake sediments, New Zealand, J. Paleolimnol., 11, 333–348, 1994.

Parajka, J., Kohnová, S., Bálint, G., Barbuc, M., Borga, M., Claps, P., Cheval, S., Dumitrescu, A., Gaume, E., Hlavčová, K., Merz, R., Pfaundler, M., Stancalie, G., Szolgay, J., and Blöschl, G.: Seasonal characteristics of flood regimes across the Alpine–Carpathian range, J. Hydrol., 394, 78–89, 2010.

Passega, R.: Grain-size representation by CM patterns as a geological tool, J. Sediment. Petrol., 34, 830–847, 1964.

Plaut, G., Schuepbach, E., and Doctor, M. Heavy precipitation events over a few Alpine sub-regions and the links with large-scale circulation, 1971–1995, Clim. Res., 17, 285–302, 2009.

Raible, C. C., Yoshimori, M., Stocker, T. F., and Casty, C.: Extreme midlatitude cyclones and their implications for precipitation and wind speed extremes in simulations of the Maunder Minimum versus present day conditions, Clim. Dynam., 28, 409–423, 2007.

Rajczak, J., Pall, P., and Schär, C.: Projections of extreme precipitation events in regional climate simulations for Europe and the Alpine Region, J. Geophys. Res. Atm., 118, 1–17, 2013.

Reimer, P. J., Bard, E., Bayliss, A., Beck, J. W., Blackwell, P. G., Bronk Ramsey, C., Buck, C. E., Cheng, H., Edwards, R. L., Friedrich, M., Grootes, P. M., Guilderson, T. P., Haflidason, H., Hajdas, I., Hatt, C., Heaton, T. J., Hogg, A. G., Hughen, K. A., Kaiser, K. F., Kromer, B., Manning, S. W., Niu, M., Reimer, R. W., Richards, D. A., Scott, E. M., Southon, J. R., Turney, C. S. M., and van der Plicht, J.: IntCal13 and MARINE13 radiocarbon age calibration curves 0–50000 years calBP, Radiocarbon, 55, 1869–1887, 2013.

Russell, J. M., Vogel, H., Konecky, B. L., Bijaksana, S., Huang, Y., Melles, M., Wattrus, N., Costa, K., and King, J. W.: Glacial forcing of central Indonesian hydroclimate since 60,000 y B.P., Proc. Nat. Acad. Sci., 111, 5100–5105, 2014.

Sauerbrey, M. A., Juschus, O., Gebhardt, A. C., Wennrich, V., Nowaczyk, N. R., and Melles, M.: Mass movement deposits in the 3.6 Ma sediment record of Lake El'gygytgyn, Far East Russian Arctic, Clim. Past, 9, 1949–1967, doi:10.5194/cp-9-1949-2013, 2013.

Schiefer, E., Gilbert, R., and Hassan, M. A.: A lake sediment-based proxy of floods in the Rocky Mountain Front Ranges, Canada, J. Paleolimnol., 45, 137–149, 2011.

Schulte, L., Peña, J. C., Carvalho, F., Schmidt, T., Julià, R., Llorca, J., and Veit, H.: A 2600-year history of floods in the Bernese Alps, Switzerland: frequencies, mechanisms and climate forcing, Hydrol. Earth Syst. Sci., 19, 3047–3072, doi:10.5194/hess-19-3047-2015, 2015.

Schwartz, S., Tricart, P., Lardeaux, J. M., Guillot, S., and Vidal, O.: Late tectonic and metamorphic evolution of the Piedmont accretionary wedge(Queyras Schistes lustrés, western Alps): Evidences for tilting during Alpine collision, Geol. Soc. Ame. Bull., 121, 502–518, 2009.

Scotti, O., Baumont, D., Quenet, G., and Levret, A.: The French macroseismic database SISFRANCE: objectives, results and perspectives, Ann. Geophys., 47, 571–581, 2004.

Servonnat, J., Yiou, P., Khodri, M., Swingedouw, D., and Denvil, S.: Influence of solar variability, CO_2 and orbital forcing between 1000 and 1850 AD in the IPSLCM4 model, Clim. Past, 6, 445–460, doi:10.5194/cp-6-445-2010, 2010.

Simonneau, A., Chapron, E., Vannière, B., Wirth, S. B., Gilli, A., Di Giovanni, C., Anselmetti, F. S., Desmet, M., and Magny, M.: Mass-movement and flood-induced deposits in Lake Ledro, southern Alps, Italy: implications for Holocene palaeohydrology and natural hazards, Clim. Past, 9, 825–840, doi:10.5194/cp-9-825-2013, 2013.

Sivan, O., Miramont, C., Pichard, G., and Prosper-Laget, V. : Les conditions climatiques de la torrentialité au cours du Petit Age Glaciaire de Provence, Archeologie du Midi Medieval, 26, 157–168, 2009.

Stockmarr, J.: Tablets with spores used in absolute pollen analysis, Pollen Spores, 13, 615–621, 1971.

Støren, E. N., Olaf Dahl, S., Nesje, A., and Paasche Ø.: Identifying the sedimentary imprint of high-frequency Holocene river floods in lake sediments: development and application of a new method, Quaternary Sci. Rev., 29, 3021–3033, 2010.

Strasser, M., Hilbe, M., and Anselmetti, F. S.:, Mapping basin-wide subaquatic slope failure susceptibility as a tool to assess regional seismic and tsunami hazards, Mar. Geophys. Res., 32, 331–347, 2011.

Sturm, M. and Matter, A.: Turbidites and varves in Lake Brienz (Switzerland): deposition of clastic detritus by density currents, Int. Assoc. Sedimentol. Spec. Publ., 2, 147–168, 1978.

Swierczynski, T., Lauterbach, S., Dulski, P., Delgado, J., Merz, B., and Brauer, A.: Mid- to late Holocene flood frequency changes in the northeastern Alps as recorded in varved sediments of Lake Mondsee (Upper Austria), Quaternary Sci. Rev., 80, 78–90, 2013.

Thorndycraft, V. R. and Benito, G.: Late Holocene chronology of Spain: the role of climatic variability and human impact, Catena, 66, 34–41, 2006.

Torres, N. T., Och, L. M., Hauser, P. C., Furrer, G., Brandl, H., Vologina, E., Sturm, M., and Bürgmann, H., and Müller, B.: Early diagenetic processes generate iron and manganese oxide layers in the sediments of Lake Baikal, Siberia, Env. Sci., 16, 879–889, 2014.

Trigo, I. F. and Davies, T. D.: Decline in Mediterranean rainfall caused by weakening of Mediterranean cyclones, Geophys. Res. Lett., 27, 2913–2916, 2000.

Van Daele, M., Versteeg, W., Pino, M., Urrutia, R., and De Batist, M.: Widespread deformation of basin-plain sediments in Aysén fjord [Chile] due to impact by earthquake-triggered, onshore-generated mass movements, Marine Geol., 337, 67–79, 2013.

Van Daele, M., Moernaut, J., Doom, L. , Boes, E. , Fontijn, K., Heirman, K. , Vandoorne, W., Hebbeln, D., Pino, M., Urrutia, R., Brümmer, R., and De Batist, M.: A comparison of the sedimentary records of the 1960 and 2010 great Chilean earthquakes in 17 lakes: Implications for quantitative lacustrine palaeoseismology, Sedimentology, 62, 1466–1496, 2015.

Van Geel, B. and Aptroot, A.: Fossil ascomycetes in Quaternary deposits, Nova Hedwig, 82, 313–329, 2006.

Van Geel, B., Buurman, J., Brinkkemper, O., Schelvis, J., Aptroot, A., van Reenen, G., and Hakjbilj, T.: Environmental reconstruction of a Roman period settlement site in Uitgeest (The Netherlands), with special reference to coprophilous fungi, J. Archaeol. Sci., 30, 873–883, 2003.

Wilhelm, B., Arnaud, F., Sabatier, P., Crouzet, C., Brisset, E., Chaumillon, E., Disnar, J. R., Guiter, F., Malet, E.,Reyss, J. L., Tachikawa, K., Bard, E., and Delannoy, J. J.: 1400 years of ex-

treme precipitation patterns over the Mediterranean French Alps and possible forcing mechanisms, Quaternary Res., 78, 1–12, 2012a.

Wilhelm, B., Arnaud, F., Enters, D., Allignol, F., Legaz, A., Magand, O., Revillon, S., Giguet-Covex, C., and Malet, E.: Does global warming favour the occurrence of extreme floods in European Alps? First evidences from a NW Alps proglacial lake sediment record, Clim. Change., 113, 563–581, 2012b.

Wilhelm, B., Arnaud, F., Sabatier, P., Magand, O., Chapron, E., Courp, T., Tachikawa, K., Fanget, B., Malet, E., Pignol, C., Bard, E., and Delannoy, J. J.: Palaeoflood activity and climate change over the last 1400 years recorded by lake sediments in the NW European Alps, J. Quat. Sci., 28, 189–199, 2013.

Wilhelm, B., Sabatier, P., and Arnaud, F.: Is a regional flood signal reproducible from lake sediments?, Sedimentology, 62, 1103–1117, 2015.

Wirth S. B., Glur, L., Gilli, A., and Anselmetti, F. S.: Holocene flood frequency across the Central Alps – solar forcing and evidence for variations in North Atlantic atmospheric circulation, Quaternary Sci. Rev., 80, 112–128, 2013a.

Wirth, S. B., Gilli, A., Simonneau, A., Ariztegui, D., Vannière, B., Glur, L., Chapron, E., Magny, M., and Anselmetti, F. S.: A 2000-year long seasonal record of floods in the southern European Alps, Geophys. Res. Let., 40, 4025–4029, 2013b.